ORNL-TM-4992

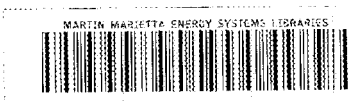

ANALYSIS OF STRESS-STRAIN BEHAVIOR OF TYPE 316 STAINLESS STEEL

Dieter Fahr

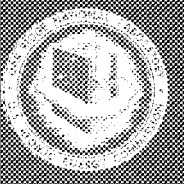

OAK RIDGE NATIONAL LABORATORY
OPERATED BY UNION CARBIDE CORPORATION • FOR THE U.S. ATOMIC ENERGY COMMISSION

Printed in the United States of America. Available from
National Technical Information Service
U.S. Department of Commerce
5285 Port Royal Road, Springfield, Virginia 22151
Price: Printed Copy $4.00; Microfiche $1.45

ORNL-TM-4292
UC-79b, -79h, and -79k

Contract No. W-7405-eng-26

METALS AND CERAMICS DIVISION

ANALYSIS OF STRESS-STRAIN BEHAVIOR OF TYPE 316 STAINLESS STEEL

Dieter Fahr

NOVEMBER 1973

OAK RIDGE NATIONAL LABORATORY
Oak Ridge, Tennessee 37830
operated by
UNION CARBIDE CORPORATION
for the
U.S. ATOMIC ENERGY COMMISSION

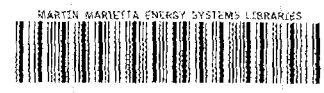

CONTENTS

ANALYSIS OF STRESS-STRAIN BEHAVIOR OF TYPE 316 STAINLESS STEEL

Dieter Fahr

ABSTRACT

Engineering stress-strain curves of annealed, cold-worked, and aged type 316 stainless steel were analyzed qualitatively. Atom-defect interactions were related to work-hardening rates and tensile data on the basis of serrations occurring in such stress-strain curves. Three types of serrations have been identified. The effect of varying strain rate was studied by varying crosshead speeds from 0.002 to 2 in./min in room-temperature tests and tests at 650°C. Only at 650°C had the crosshead speed a significant influence on the ultimate tensile strength and uniform plastic strain; yield strength and elongation values varied little with strain rate. The effect of test temperature ranging from 450 to 650°C was studied on as-annealed, annealed and aged, 20% cold-worked, and cold-worked and aged specimens. Specimens aged for 4000 hr were tested at their aging temperatures. Long-term aging at 450 and 550°C had little or no effect on mechanical-property data of as-annealed specimens, but affected those of previously cold-worked specimens measurably. Aging as-annealed specimens for 4000 hr at 450°C did not lead to precipitation; at 550°C grain boundary precipitation took place; and at 650°C many precipitate particles crystallographically related to the matrix could be observed within the grains and at their boundaries. This precipitate structure led to an increased yield strength and was markedly different from that found in the recrystallized portion of cold-worked specimens aged at 650°C. Cold work facilitated precipitation and the formation of large σ-phase particles. Some results of the effect of short-time (10-hr) aging on room-temperature tensile data, and of the influence of varying amounts of tensile prestrain on tensile data of specimens subsequently aged 4000 hr *and* tested at 650°C, are also included.

INTRODUCTION

Good high-temperature mechanical properties and adequate corrosion resistance make type 316 stainless steel an attractive candidate for nuclear reactor applications. Mechanical-property changes during neutron irradiation are due to microscopic and submicroscopic changes in the defect structure and alloy composition (transmutation products and radiation-induced precipitation). In order to better understand and interpret the effects of neutron irradiation on the mechanical behavior of reactor components, a thorough understanding of the behavior characteristics of unirradiated material is necessary. For this reason, an attempt was made to correlate microscopic processes with the stress-strain behavior of type 316 stainless steel at elevated temperatures. As-annealed and cold-worked specimens were tested in aged and unaged conditions at different temperatures and strain rates.

Although fcc metals and alloys are usually less sensitive to changes in strain rate and temperature than bcc alloys, their deformation characteristics change measurably with the above variables when diffusion-controlled atom-atom, atom-defect, or defect-defect interactions occur. Phenomena such as serrations in stress-strain curves actually reveal such interactions taking place during the test and should be considered in the subsequent evaluation of mechanical-property data. An understanding of the phenomena involved and their mutual interactions during processing and testing will enable one to extrapolate and predict mechanical behavior for similar alloys and other conditions. Actual testing conditions are seldom representative of those to be encountered by the material in service, and this is especially true for tensile tests.

Serrations in stress-strain curves are observed in many alloys, and, depending on the alloy and test conditions, they may be due to short-range-order hardening,[1] vacancy hardening,[2] creation of stacking faults,[3] martensitic phase transformations, and other mechanisms. The serrations observed in the present

1. R. W. Cahn, "Correlation of Local Order with Mechanical Properties," Chap. 6, pp. 179–213 in *Proc. Symposium on Local Atomic Arrangements Studied by X-ray Diffraction*, Gordon and Breach, New York, 1965.
2. H. Green and N. Brown, *Trans. AIME* 197, 1240–44 (1953).
3. C. H. White and R. W. K. Honeycombe, *J. Iron Steel Inst.* 200, 457–66 (1962).

study of type 316 stainless steel are attributed to the interaction of interstitial carbon and nitrogen atoms with dislocations. Thus, the serrations are a function of the test temperature (diffusion rate), strain rate (diffusion depends on time), strain (dislocation density), stress (average dislocation velocity), alloy content (affects thermodynamic activity, and thus diffusion rate, and determines the quantity of interstitial atoms available for interaction with dislocations), aging treatments (carbon, nitrogen, and other elements may form precipitates, and thus their interactions with dislocations will be altered), and several other factors. Most of these factors can be separated experimentally, and their study, therefore, should supply answers to questions such as why and under what conditions serrations occur and what significance their amplitude, frequency, and actual shapes have. Such a study should be especially useful when compared with irradiated specimens, where the increased vacancy concentrations, as well as possible radiation-induced precipitation (depleting the matrix of carbon and nitrogen), will be reflected in the appearance of the serrations.

EXPERIMENTAL PROCEDURE

Buttonhead specimens with a gage length of 1 in. and a diameter of 0.125 in. were machined from 0.26-in.-diam rods of AISI type 316 stainless steel, the composition of which is given in Table 1. All rods were annealed in argon for 1 hr at 1200°C and reduced 50% in area by swaging at room temperature. Specimens to be tested in the annealed condition were annealed for 1 hr at 1050°C (in argon) after swaging. Specimens to be tested in the cold-worked condition were machined after annealing for 1 hr at 1050°C (in argon) and subsequent reduction in area (20%) by swaging. Specimens to be aged were encapsulated in stainless steel containers and aged (in static argon) for 4000 hr at 450, 550, and 650°C. Short-time aging treatments (10 hr) were performed in an argon-purged furnace. Tensile tests were conducted in air at temperatures ranging from 350 to 750°C using an Instron testing machine at crosshead speeds from 0.002 to 2 in./min. Aged specimens were tested at their respective aging temperatures.

Table 1. Chemical composition of type 316 stainless steel

Element	Content (wt %)
C	0.05
N	0.05
S	0.01
P	0.01
Si	0.8
Mn	1.9
Cr	18.0
Mo	2.6
Ni	13.0
Fe	Balance

EXPERIMENTAL RESULTS AND DISCUSSION

Discontinuous Yielding

The Portevin-LeChatelier effect[4] or the phenomenon of repeated or discontinuous yielding during a tensile test has been attributed to dynamic strain aging, and the solute responsible is considered to diffuse

4. A. Portevin and F. LeChatelier, *C. R. Acad. Sci.* **176**, 507–10 (1923).

fast enough to slow down freely moving dislocations by forming an atmosphere or "cloud"[5] around them. Eventually, the stress rises sufficiently to cause the dislocations to break away from their solute atmospheres and/or to generate new dislocations. This process is then repeated. Accordingly, dislocation movement oscillates between fast and slow motion, and a serrated stress-strain curve is observed.

The manifold and complex appearance of such serrations is the main reason so many researchers find it more convenient to ignore them than to correlate their shape, amplitude, and frequency with processes on an atomic scale. It is, however, possible to ascribe different types of serrations to different atom-defect interactions within an alloy if the processing and testing conditions are known.

Classification of Serrations

By careful analysis and comparison of the original load-elongation graphs and the respective test temperatures and strain rates, it is possible to distinguish three types of serrations due to significantly different micromechanisms. Figure 1 shows typical portions of stress-strain curves, as obtained in this investigation. Such curves more often than not contain combinations of two and, under certain conditions, even all three types of serrations. Russell[6] was the first to distinguish between two types of serrations, A and B, studying repeated yielding in tin bronze alloys. Soler-Gomez and Tegart,[7] studying serrated flow in gold-indium alloys, also found type A serrations as well as a new serration, type C. While the serrations in the above studies were due to interactions between mobile dislocations and substitutionally dissolved solute atoms, discontinuous yielding in type 316 stainless steel is caused by interactions between interstitially dissolved elements, such as carbon and nitrogen, and mobile dislocations.

Type A

Type A yielding is characterized by widely spaced yield points that increase in size and spacing as the plastic strain increases (Fig. 1).

Type A serrations are sometimes referred to as locking serrations. They are observed when test conditions allow formation of solute atmospheres that are large enough to prevent unpinning. The yield drops must, therefore, be considered due to the creation of new dislocations. The deformation process has been found to be nonhomogeneous and occurs by the formation and propagation of deformation bands along the gage section. Every time a deformation band passes down the gage length it requires a

5. A. H. Cottrell and B. A. Bilby, *Proc. Phys. Soc., London Ser. A* **62**, 49–62 (1949).
6. B. Russell, *Phil. Mag.* 8, 615–30 (1963).
7. A. J. R. Soler-Gomez and W. J. McG. Tegart, *Phil. Mag.* **20**, 495–509 (1969).

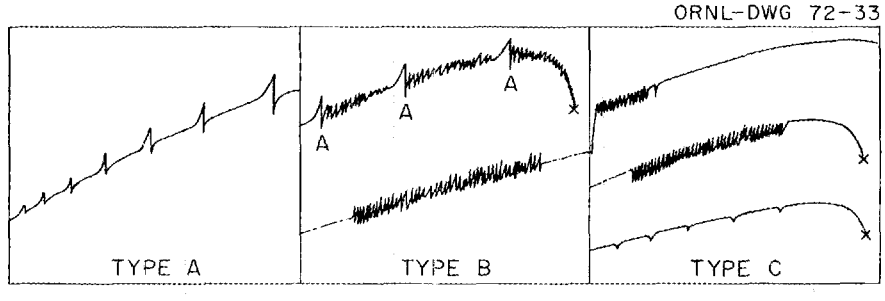

Fig. 1. Classification of discontinuous yield points in type 316 stainless steel as types (*a*) A, (*b*) B alone (bottom) and combined with A, and (*c*) C.

significantly higher stress to trigger a second deformation band than would be necessary under normal work-hardening conditions, provided the aging time is sufficient for dislocations to get locked. The spacing of type A serrations depends, thus, on the instantaneous gage length, which increases with strain. Moreover, the frequency of type A serrations depends also on temperature and time, that is to say, strain rate. If the strain rate is too high for locking to take place at a given temperature, no serrations will occur due to the above mechanism. On the other hand, if the temperature were increased, the ensuing higher diffusion rate of carbon and nitrogen atoms would make locking serrations possible even at a relatively high strain rate.

While dynamic strain aging refers to segregation of solute atoms to moving dislocations, type A serrations occur when solute atoms cannot affect the dislocations within the narrow deformation band. Thus, type A serrations do not reflect interactions between solute atoms and dislocations directly, but are due to the resulting increase in stress required for the formation of a new deformation band.

Type B

Type B yield drops, in contrast to type A yield points, are not considered to be due to formation of new deformation bands, but are believed to be the result of jerky propagation of such bands. Type B serrations occur when the fast-moving dislocations within the deformation band are affected by dynamic strain aging. Such a condition requires a higher minimum diffusion coefficient, or, in other words, B-type serrations usually occur at higher temperatures and lower strain rates than type A serrations and often in combination with them. Segregation of solute atoms to moving dislocations within the deformation band occurs most likely when a sudden increase in the density of mobile dislocation results in a corresponding decrease in the average dislocation velocity required to maintain the imposed strain rate. As a result, the moving dislocations are slowed down and locked in position almost as rapidly as they are generated, and the stress increases, deforming the specimen elastically, until a new avalanche of mobile dislocations is made available for the deformation band to propagate. This process is then repeated until a new deformation band forms because the band or bands within which the deformation had taken place either traversed the entire gage length or ran into another band. Thus, type B serrations are due to alternating elastic and plastic deformations.

Type C

Figure 1 shows that type C serrations are characterized by having yield drops that are always *below* the general level of the stress-strain curve, in contrast to type A and B serrations, which oscillate *above and below* the curve. Type C serrations are considered to result from dislocation unlocking and usually occur only when the minimum solute diffusion coefficient is higher than that required for type B serrations. In other words, type C serrations require test conditions that would actually result in no serrations when the deformation is homogeneous, for the diffusion rate of the solute must be high enough for it to migrate with the dislocations in the deformation band. However, when the deformation is inhomogeneous because of stress concentrations at grain boundaries or nonuniform cross-sectional area of the specimen, small regions of the gage sections will deform at a strain rate greater than the overall strain rate. This results in an increased drag of the atmospheres on the dislocations, which, however, does not lead to a measurable stress increase but instead causes the dislocations to break away from their atmospheres. The sudden availability of many "free" dislocations decreases the stress, which, in turn, lowers the average dislocation velocity in the deformation band so that the relatively fast-moving solute atoms can relock the dislocations temporarily for the process to be repeated. This results in very strain-rate dependent type C serrations.

Type B serrations were assumed to be due to interactions of solute atoms with mobile dislocations. Type C serrations are seen replacing type B serrations with increasing strain or temperature, or decreasing strain rate. Thus, they cannot coexist as can types A and B serrations, and they, therefore, cannot be connected with either formation or propagation of a deformation band. The continuous deformation band

akin to a Lüders band ceases to exist when type C serrations begin forming. In a transitional situation where type B serrations precede type C yield drops, type C serrations may temporarily act like propagation serrations until the deformation band front has been "smoothed" out. From this point on, deformation is not concentrated any more in a narrow localized zone at the front of the band but can virtually occur over the entire gage section simultaneously. The elimination of a narrow deformation zone drastically lowers the effective strain rate and, thus, the average dislocation velocity to the extent that the solute atmospheres can be dragged along. This explains the sudden disappearance of serrations in the stress-strain curve [Fig. 1(c)].

The results to be discussed below actually reveal even a fourth type of serrations, which could be called type D, since it can be observed at lower temperatures than type A. The mechanism and appearance are, however, very similar to those of type C serrations, so that it was decided not to extend the above classification, although Soler-Gomez and Tegart[7] stated that type C serrations can occur only at high temperatures.

Unlocking of more or less immobile dislocations can, however, occur at relatively low temperatures simply as a result of the increasing stress due to work-hardening and very limited formation of atmospheres. This is possible because the atmospheres are relatively small at low temperatures, and not much stress is required for the dislocations to break away.

The yield drops are always below the general level of the stress-strain and are separated from one another by a considerable amount of strain as are the type A yield drops. The separation also increases with increasing strain, however, not because the instantaneous gage length increases, but rather on account of an increase in the instantaneous diffusion rate, which permits the formation of larger solute atmospheres, and thus requires a higher stress level for dislocations to break away. At a constant work-hardening rate, higher stress levels can be reached only with larger strains.

Effect of Different Strain Rates

Although body-centered cubic metals and alloys are very sensitive to changes in strain rate, face-centered cubic metals or alloys, such as type 316 stainless steel, are very little affected. Tensile data of 50%-cold-worked specimens tested at room temperature and as-annealed specimens tested at 650°C are listed in Table 2 for crosshead speeds varying from 0.002 to 2 in./min.

Table 2. Tensile data of cold-worked[a] and annealed[b] type 316 stainless steel at various crosshead speeds

Crosshead speed (in./min)	Strength (psi)		Uniform plastic strain (%)	Elongation (%)
	Yield (0.2% offset)	Ultimate tensile		
	$\times 10^3$	$\times 10^3$		
Cold-Worked Material Tested at Room Temperature				
0.002	157.7	158.7	1.9	13.1
0.020	148.0	159.8	6.7	14.1
0.200	151.3	160.7	2.1	12.5
2.000	161.3	164.0	3.9	10.0
Annealed Material Tested at 650°C				
0.002	17.3	56.8	22.7	36.6
0.020	17.2	65.1	31.0	38.3
0.200	17.0	67.6	31.3	37.1
2.000	21.1	68.8	28.6	34.0

[a]Swaged at room temperature to 50% reduction in area.
[b]Annealed for 1 hr at 1050°C.

The increase in yield strength, presumably due to this 1000-fold increase in crosshead speed, was for each condition less than 4000 psi. While the yield strength was practically unaffected, changes in ultimate tensile strength occurred as soon as diffusion and, thus, time-dependent processes played a role. The most drastic change would be expected when recrystallization could take place during the test. But even in annealed specimens, significant changes can be observed. For instance, a change in crosshead speed from 0.002 to 0.020 in./min at 650°C resulted in no change in yield strength (Table 2) but in an increase in ultimate tensile strength of about 8000 psi. This was due to an increase in work-hardening rate as a result of interactions between mobile dislocations and mobile solute atoms, which are revealed by serrations in the respective stress-strain curves. Figure 2 shows 650°C stress-strain curves of as-annealed specimens tested at different crosshead speeds. Comparison of the four curves reveals excellent agreement with the above-discussed mechanisms. At the lowest strain rate (longest time for diffusion to occur), only unlocking or C-type serrations were observed; they abruptly disappeared after about 2.5% strain [Fig. 2(*a*)], because the instantaneous diffusion coefficient was high enough to allow the carbon and nitrogen atoms to migrate with about the same velocity as the average dislocation in the deformation band. The work-hardening rate was low, since relatively few dislocations were immobilized, and there was no need for large numbers of new dislocations to accommodate the strain. When the crosshead speed was increased to 0.02 in./min (essentially corresponding to a temperature decrease), type C serrations occurred only at large strains preceded by type B serrations and again stopped forming abruptly as the specimen was strained even further [Fig. 2(*b*)]. At a crosshead speed of 0.2 in./min [Fig. 2(*c*)], type A serrations first formed alone and, at larger strains, in combination with B-type serrations. When the crosshead speed was finally increased to 2 in./min [Fig. 2(*d*)], a marked change was noted. With increased strain rate the frequency and the amplitude of serrations decreased and the serrations became ill-defined [Fig. 2(*d*)].

After about 15% strain, the work-hardening rates of specimens pulled at crosshead speeds of 0.02 in./min and above (at 650°C) were clearly higher than that of the specimen pulled at 0.002 in./min, as reflected by higher uniform plastic strains and ultimate tensile strengths (Table 2), as well as the more extensive serrations of their respective stress-strain curves (Fig. 2).

The more serrated a stress-strain curve is for a specimen, the higher its work-hardening rate and its dislocation density are for a given amount of strain. This has been substantiated by electron microscopy[8,9]

8. B. A. Wilcox and G. C. Smith, *Acta Met.* **12**, 371–76 (1964).
9. J. W. Edington and R. E. Smallman, *Acta Met.* **12**, 1313–28 (1964).

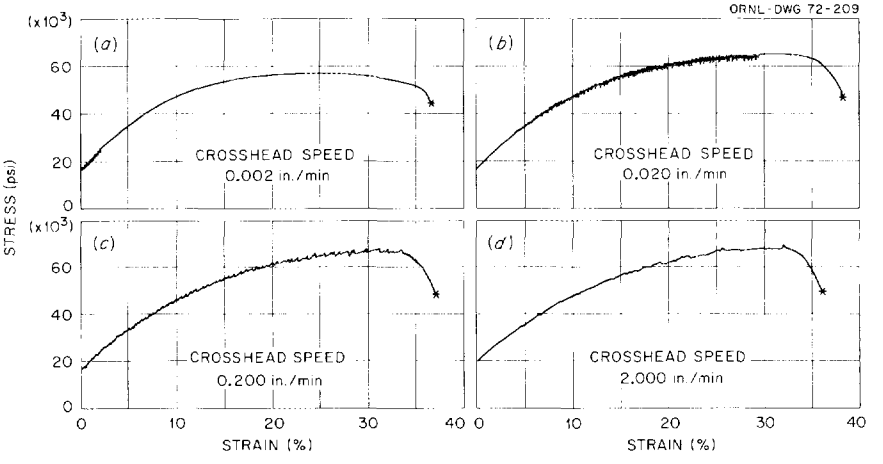

Fig. 2. Engineering stress-strain curves of type 316 stainless steel specimens annealed for 1 hr at 1050°C and tested at 650°C at various crosshead speeds.

and is considered due to the fact that more new dislocations have to be generated to accommodate the strain when the originally mobile dislocations are locked by solute atmospheres.

Effect of Different Test Temperatures

Specimens in the Annealed Condition

Tensile data of specimens annealed for 1 hr at 1050°C and tested at various temperatures from 350 to 750°C are listed in Table 3. While the yield strengths of the annealed specimens hardly varied with temperature up to 750°C, the ultimate tensile strength and uniform plastic strain values dropped off rapidly above 550°C (Fig. 3). Both measures reflect the work-hardening rate, which remained essentially the same between 350 and 550°C. The stress-strain curves for these test temperatures [Fig. 4(*a*), (*b*), (*c*)] show

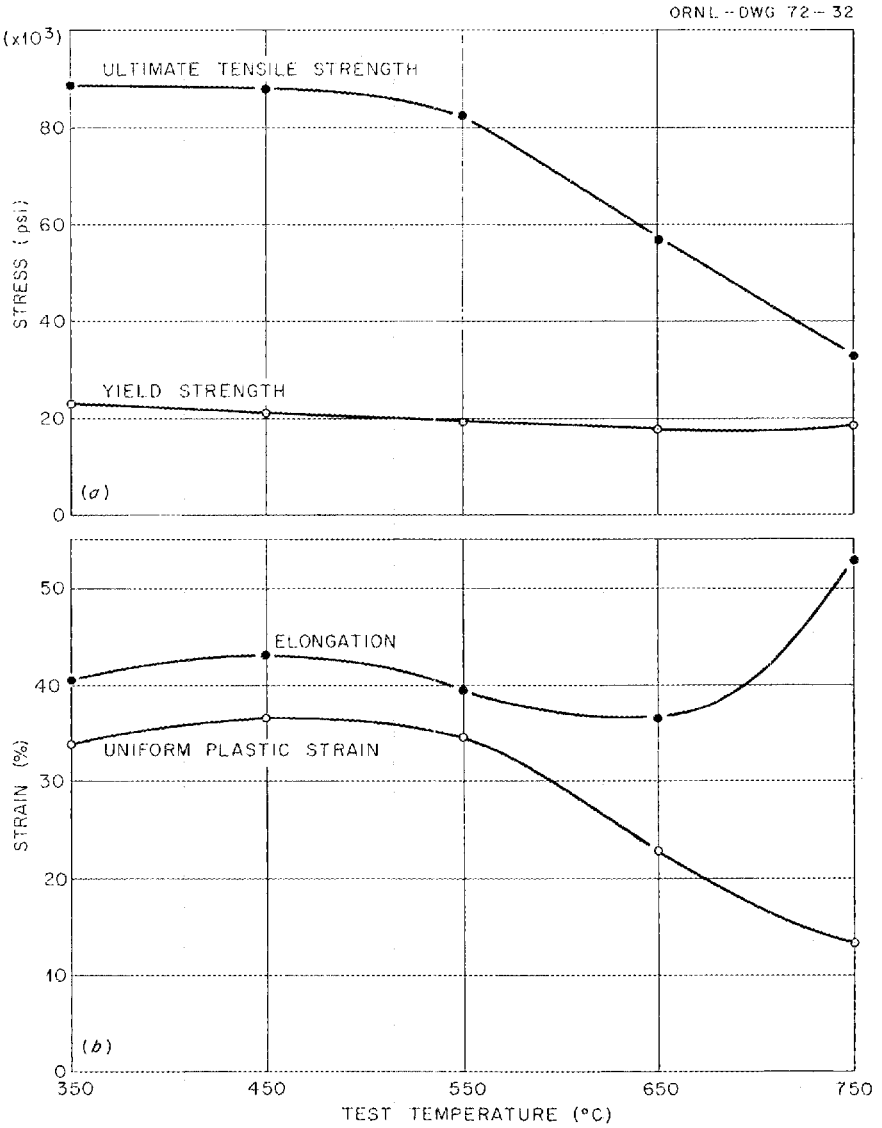

Fig. 3. Effect of test temperature on (*a*) ultimate tensile and yield strengths and (*b*) elongation and uniform plastic strain of type 316 stainless steel annealed for 1 hr at 1050°C and tested at a crosshead speed of 0.002 in./min.

Table 3. Tensile data[a] of as-annealed[b] type 316 stainless steel at various test temperatures

Test temperature (°C)	Strength (psi)		Uniform plastic strain (%)	Elongation (%)
	Yield (0.2% offset)	Ultimate tensile		
	$\times 10^3$	$\times 10^3$		
350	23.0	88.5	34.2	40.5
450	20.8	87.7	36.6	43.3
550	19.2	82.4	34.6	39.6
650	17.3	56.8	22.7	36.6
750	18.4	33.4	13.3	53.0

[a]Tested at a crosshead speed of 0.002 in./min.
[b]Annealed for 1 hr at 1050°C.

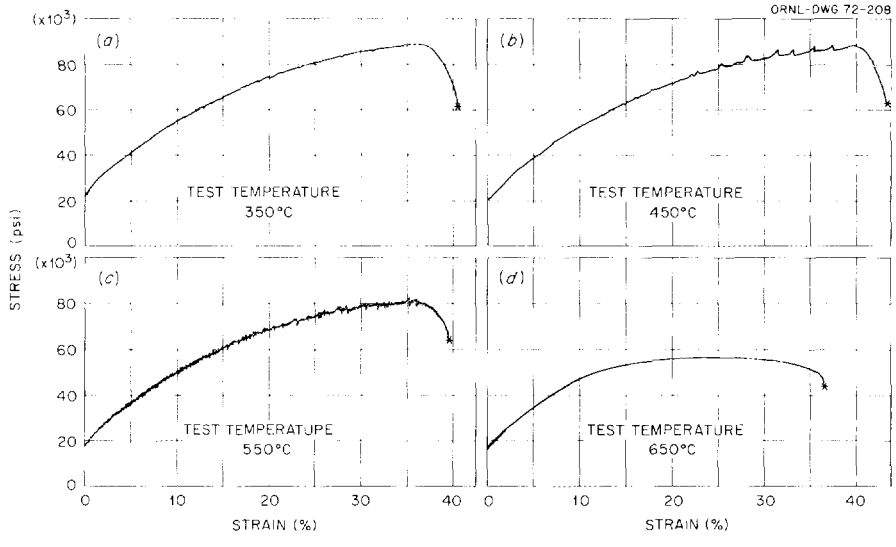

Fig. 4. Engineering stress-strain curves of type 316 stainless steel specimens annealed for 1 hr at 1050°C and tested at a crosshead speed of 0.002 in./min at various temperatures.

serrations along most of the stress-strain curve, but the stress-strain curve of the specimen tested at 650°C exhibits only some C-type serrations at very low strains. At 350°C the serrations were of the low-temperature C type, at 450°C they were of almost pure type A, and at 550°C a combination of types A and B could be seen. The tendency toward formation of atmospheres decreased rapidly with increasing temperature above 650°C; the stress-strain curve at 750°C was completely smooth.

The high elongation value at 750°C [Fig. 3(*b*)] was due to dynamic recovery. Electron microscopy has shown that 1 hr at 750°C suffices to completely recrystallize a 20%-cold-worked specimen. At a crosshead speed of 0.002 in./min, the 750°C tensile test lasted more than 4 hr.

The microstructure of the uniformly strained portion of the gage section is shown in Fig. 5 for the as-annealed specimens tested at various temperatures. No evidence can be found that precipitation took place during the tests at 350, 450, and 550°C, but grain and twin boundaries of the specimens tested at 650 and 750°C are clearly decorated with precipitates that formed during the test. Thus, not only were the carbon and nitrogen diffusion rates too high at 650 and 750°C for serrations to occur to any significant

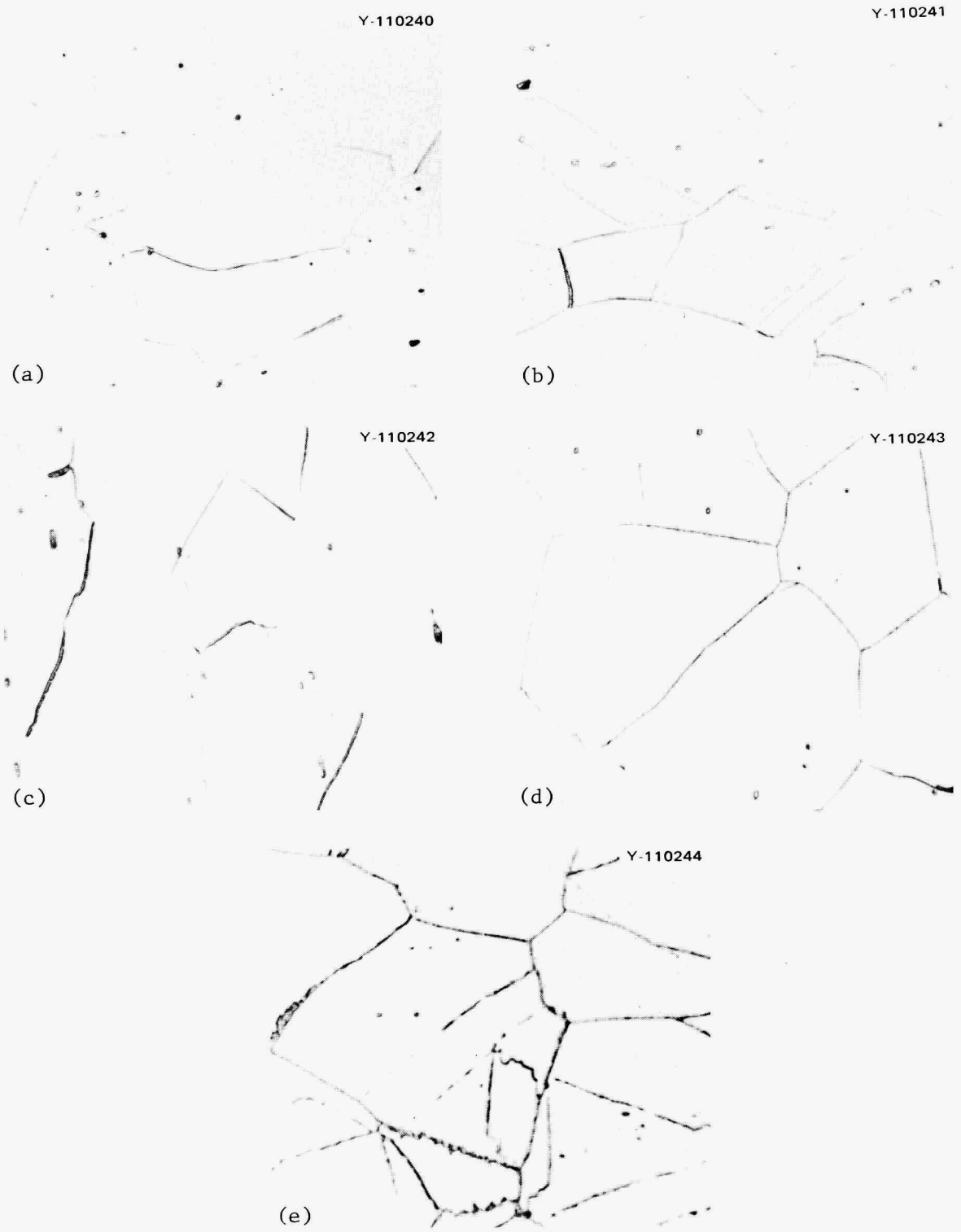

Fig. 5. Optical micrographs showing the microstructure of the uniformly strained portion of the gage section of type 316 stainless steel specimens annealed for 1 hr at 1050°C and tested at a crosshead speed of 0.002 in./min at (*a*) 350°C, (*b*) 450°C, (*c*) 550°C, (*d*) 650°C, and (*e*) 750°C. Vibratorily polished and etched (50% HCl, 33% glycerin, and 17% HNO_3) at room temperature. 750×.

extent at the given crosshead speed, but the actual amount of these elements in solution has also been reduced because of precipitation during the test.

Specimens in the Annealed-and-Aged Condition

Tensile data of specimens annealed for 1 hr at 1050°C and subsequently aged for 4000 hr *and* tested at 450, 550, and 650°C are listed in Table 4. A comparison of the data in Tables 3 and 4 reveals that long-time aging at 450 and 550°C has practically no effect on the mechanical properties. The yield strengths are slightly higher in the unaged condition, and very small amounts of precipitate that may have formed during aging were most likely responsible for their lower ultimate tensile strengths through a lower work-hardening rate. Figure 6 shows that no significant precipitation took place at 450°C, but some grain boundary precipitate formed at 550°C. Uniform plastic strain and elongation values at 450°C were higher in the unaged condition, while the specimen aged and tested at 550°C reached higher values than the corresponding unaged specimen. Aging at 650°C, however, had a significant effect on mechanical-property data: in spite of the higher test temperature, the yield strength at 650°C was about 35 to 40% higher than those of the specimens aged and tested at 550 and 450°C. It was also higher than that of the unaged specimen tested at 650°C. The precipitation structure shown in Fig. 6(*c*) must be considered responsible for this. Although the precipitates increase the yield strength, the ultimate tensile strength is for the same reason lower than in the unaged condition. Carbon and alloying elements taken out of solution reduced the work-hardening rate; this was also reflected in the uniform plastic strain value, which was only about half that of the unaged specimen, although the elongation values were practically the same.

The stress-strain curve of the specimen aged and tested at 450°C exhibits types A and B serrations. Very heavy serrations, mainly of the B type, characterize the stress-strain curve of the specimen aged and tested at 550°C. These heavy serrations, heavier than for the corresponding as-annealed specimen, are indicative of a high work-hardening rate and explain the high uniform plastic strain and elongation values [Fig. 7(*b*)]. Figure 7(*a*) shows a marked difference between ultimate tensile and yield strengths for specimens tested and aged at 450 and 550°C. This measure of work-hardening rate then dropped to about one-third of its value at lower temperatures when a specimen was tested and aged at 650°C. The sharp drop in uniform plastic strain between 550 and 650°C [Fig. 7(*b*)] also reflects the much-decreased work-hardening rate and indicates that the drastic change could not be due to a change in test temperature alone but was also caused by a significant change in microstructure. To prove this, a specimen aged for 4000 hr at 550°C was tested at 650°C, and the uniform plastic strain dropped only from 35 to 25%, although it dropped below 12% for the specimen tested *and* aged at 650°C.

Table 4. Tensile data[a] of annealed-and-aged[b] type 316 stainless steel at various test temperatures

Aging and test temperature (°C)	Strength (psi)		Uniform plastic strain (%)	Elongation (%)
	Yield (0.2% offset)	Ultimate tensile		
	$\times 10^3$	$\times 10^3$		
450	19.6	81.9	31.8	36.2
550	18.6	76.8	35.0	41.8
650	26.9	48.1	11.7	36.8

[a]Tested at a crosshead speed of 0.002 in./min.
[b]Annealed for 1 hr at 1050°C and then aged 4000 hr at the test temperature.

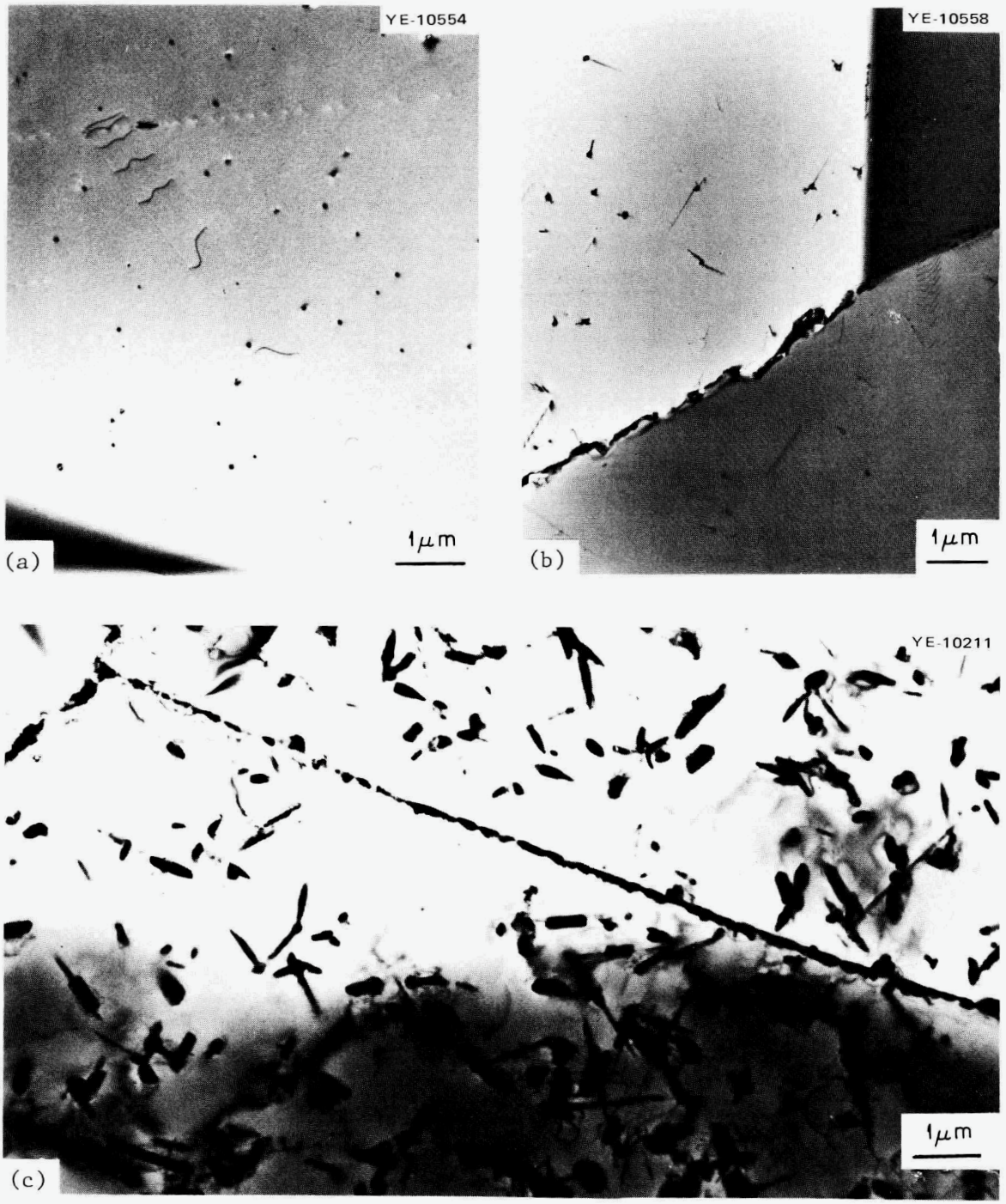

Fig. 6. Electron micrographs showing the microstructure of as-annealed (1 hr at 1050°C) type 316 stainless steel specimens aged 4000 hr at (*a*) 450, (*b*) 550, and (*c*) 650°C.

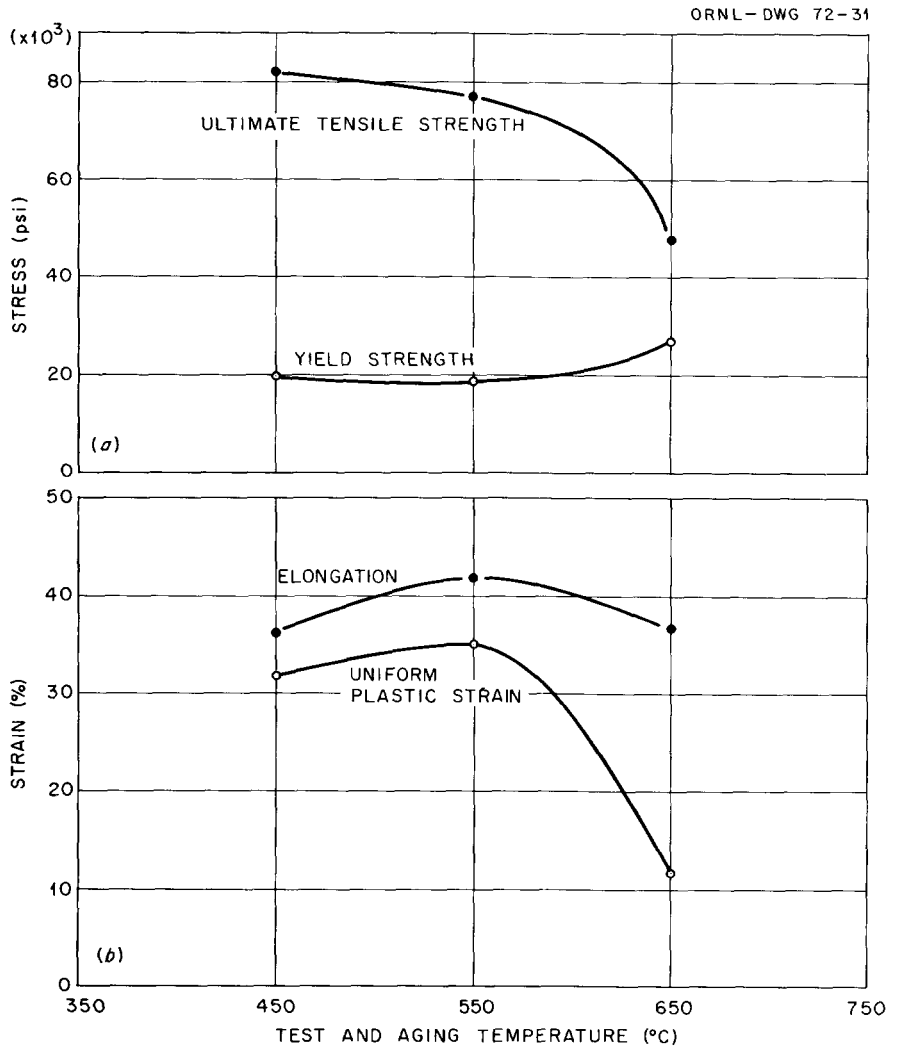

Fig. 7. Effect of test *and* aging temperature on (*a*) ultimate tensile and yield strengths, and (*b*) elongation and uniform plastic strain of type 316 stainless steel annealed 1 hr at 1050°C, aged 4000 hr at various temperatures, and tested at a crosshead speed of 0.002 in./min at the aging temperatures.

In Fig. 8, the stress-strain curves for the specimens aged at 550°C and tested at 550°C and 650°C are compared. The interactions of mobile atoms with mobile dislocations at 550°C led to the heavy serrations referred to above. The serrations are mainly of the B type combined with some of type A. At a test temperature of 650°C, only C-type serrations occurred, and the stress-strain curve became smooth at large strains. Figure 8 dramatically demonstrates the effects of interactions between solute atoms and dislocations and the validity of the model developed earlier. An increase in crosshead speed could bring about a complete reversal of the two stress-strain curves by increasing the work-hardening rate of the specimen represented by curve *A* and decreasing that of the specimen characterized by curve *B*.

Figure 9 shows to what extent the stress-strain behavior of identical specimens can be changed by increasing the crosshead speed from 0.002 to 0.2 in./min. The serration type changed from C to A, and the work-hardening rate, uniform plastic strain, and ultimate tensile strength values increased correspondingly. Thus, changes in test temperature (Fig. 8) as well as crosshead speed (Fig. 9) led to marked changes in

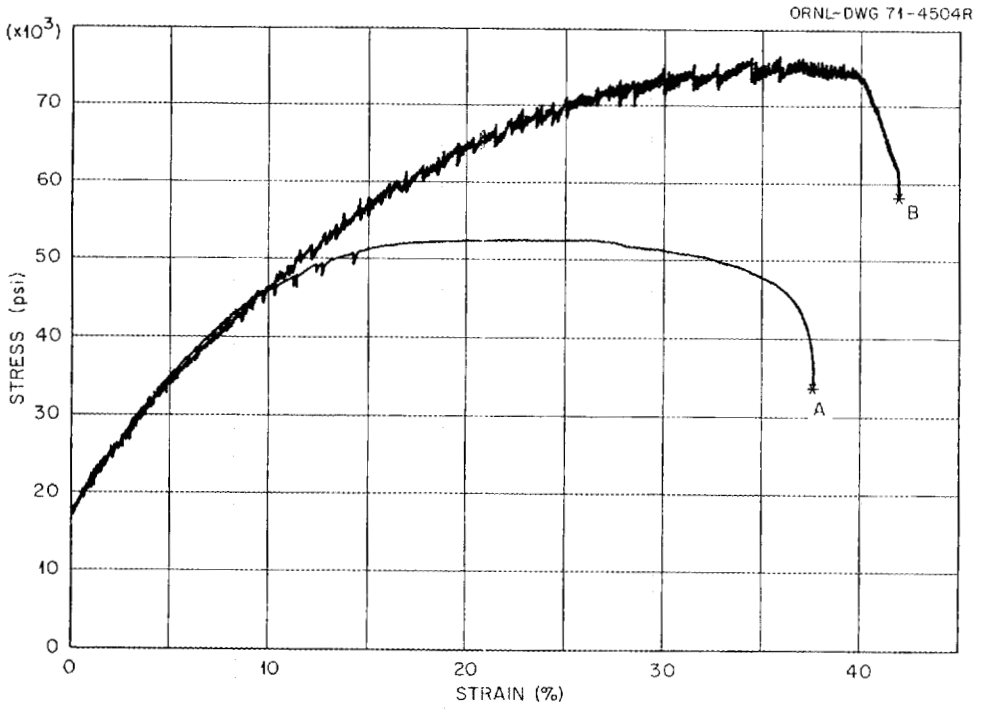

Fig. 8. Engineering stress-strain curves of type 316 stainless steel specimens annealed 1 hr at 1050°C, aged 4000 hr at 550°C, and tested at a crosshead speed of 0.002 in./min at (*A*) 650 and (*B*) 550°C.

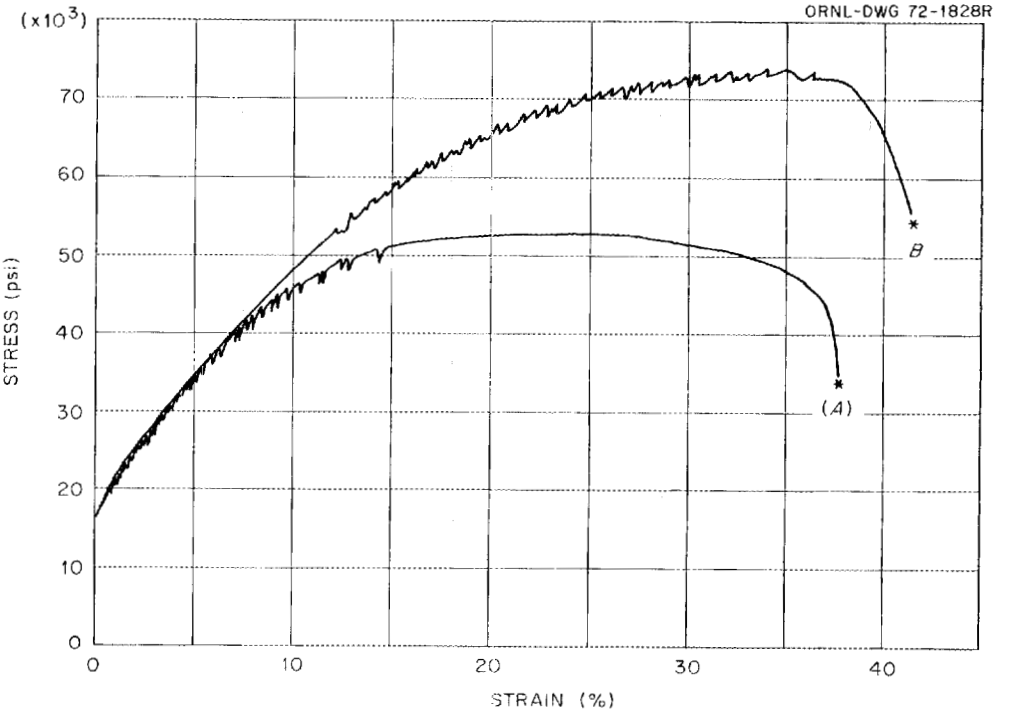

Fig. 9. Engineering stress-strain curves of type 316 stainless steel specimens annealed 1 hr at 1050°C, aged 4000 hr at 550°C, and tested at 650°C at a crosshead speed of (*A*) 0.002 and (*B*) 0.200 in./min.

ultimate tensile strength. Since the fatigue limit has been found to be a function of the ultimate tensile strength,[10] such variations may be of considerable significance.

Specimens in the Cold-Worked Condition

Tensile data of specimens reduced 20% in area by swaging at room temperature and tested at various temperatures from 350 to 650°C are listed in Table 5.

The work-hardening rate of the cold-worked specimens is very low for all test temperatures, as can be seen from the small difference between ultimate tensile and yield strengths in Fig. 10(*a*) and the low uniform plastic strain in Fig. 10(*b*). Moreover, none of the stress-strain curves exhibit any serrations, even though serrations could be found in most of the stress-strain curves of as-annealed specimens tested at corresponding temperatures (Fig. 4).

The absence of serrations in stress-strain curves of cold-worked specimens is believed to be due to the much higher stress level at which plastic deformation took place, and the resulting higher average dislocation velocity. Moreover, more carbon and nitrogen can be expected to be tied up by the much larger number of dislocations. This also facilitates precipitation on heating to the test temperature and during the test.

The tensile data presented in Fig. 10 indicate that recovery took place before and during the test at 650°C. The elongation value increased abruptly at 650°C [Fig. 10(*b*)], and the drop of both the yield and ultimate tensile strengths between 550 and 650°C was sharper for cold-worked [Fig. 10(*a*)] than for as-annealed specimens [Fig. 3(*a*)], indicating that changes in the cold-worked structure (recovery) accentuate the decline in strength due to an increased test temperature alone.

Optical micrographs of the uniformly strained portion of the gage section (Fig. 11) reveal that precipitation during the test has proceeded further in the specimen tested at 650°C [Fig. 11(*b*)] than in the specimen tested at 550°C [Fig. 11(*a*)]. A comparison of Fig. 11 with Fig. 5 also shows that precipitation occurs more readily in cold-worked than in annealed specimens.

Specimens in the Cold-Worked-and-Aged Condition

Long-time aging. Table 6 lists tensile data of specimens reduced 20% in area by swaging at room temperature and subsequently aged for 4000 hr at 450, 550, and 650°C and tested at the aging temperature.

10. C. Crussard et al., "A Comparison of Ductile and Fatigue Fractures," pp. 524–61 in *Fracture* (Proc. Intern. Conf. Atomic Mechanisms of Fracture, Swampscott, Mass., April 12–16, 1959), Technology Press, MIT, and Wiley, New York, 1959.

Table 5. Tensile data[a] of cold-worked[b] type 316 stainless steel at various test temperatures

Test temperature (°C)	Strength (psi)		Uniform plastic strain (%)	Elongation (%)
	Yield (0.2% offset)	Ultimate tensile		
	$\times 10^3$	$\times 10^3$		
350	131.3	136.8	0.6	5.1
450	129.6	136.2	0.7	5.2
550	117.9	123.7	0.9	5.4
650	78.3	84.4	1.3	21.0

[a]Tested at a crosshead speed of 0.002 in./min.
[b]Swaged at room temperature (20% reduction in area).

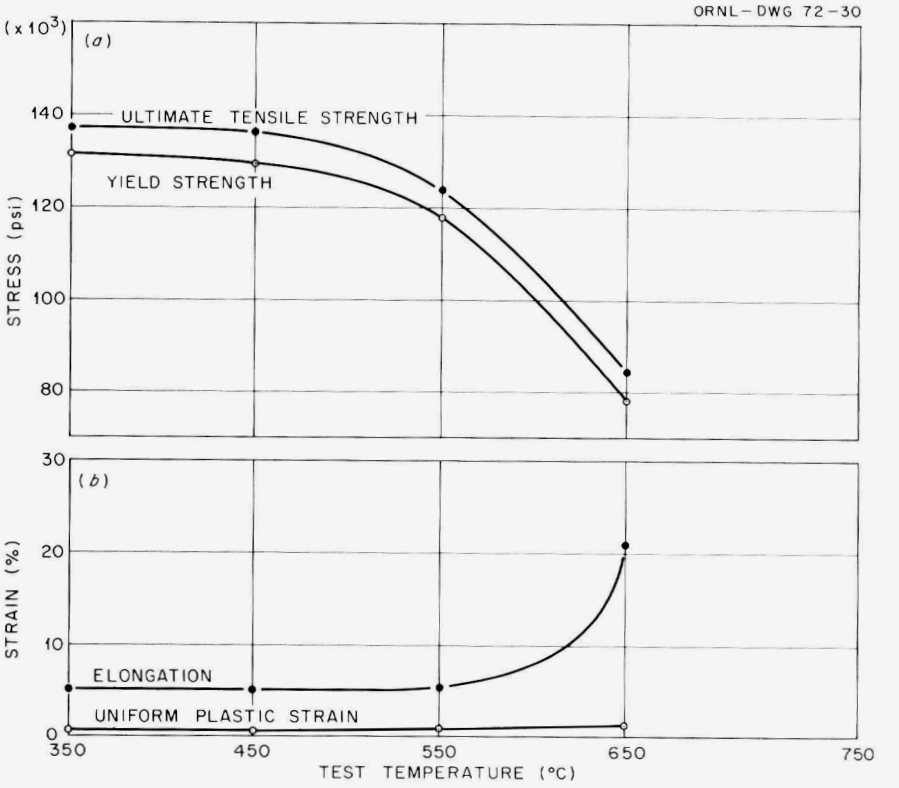

Fig. 10. Effect of test temperature on (*a*) ultimate tensile and yield strengths, and (*b*) elongation and uniform plastic strain of type 316 stainless steel specimens reduced 20% in area by swaging at room temperature and tested at a crosshead speed of 0.002 in./min.

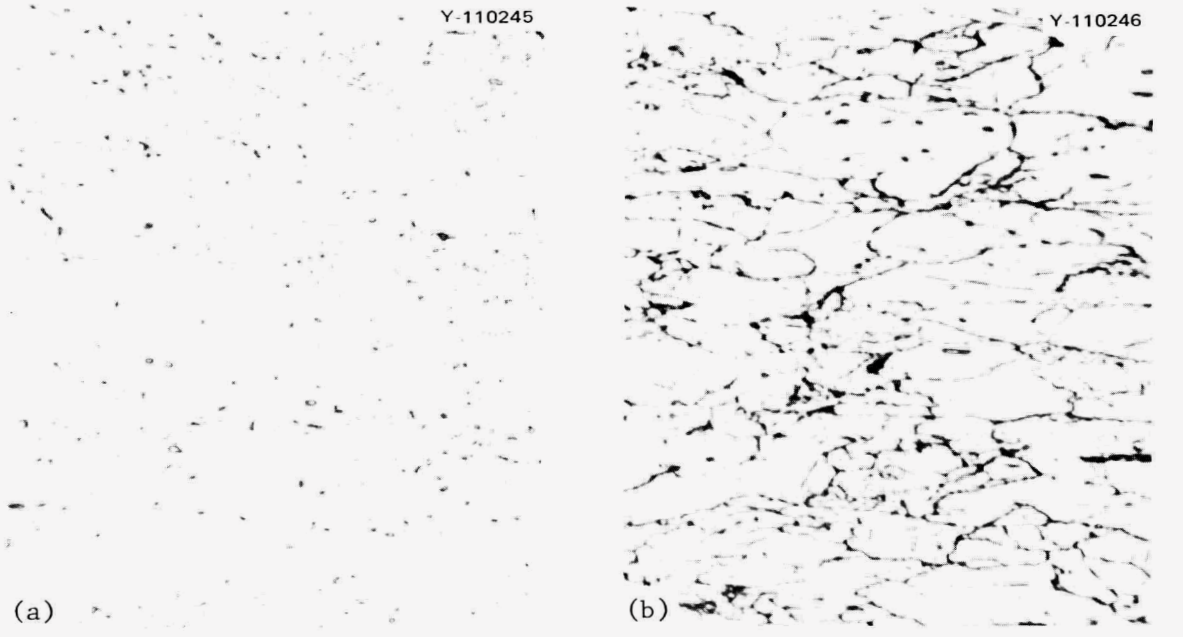

Fig. 11. Optical micrographs showing the microstructure of the uniformly strained portion of the gage section of type 316 stainless steel specimens reduced 20% in area by swaging at room temperature and tested at a crosshead speed of 0.002 in./min at (*a*) 550°C and (*b*) 650°C. Vibratorily polished and etched (50% HCl, 33% glycerin, and 17% HNO_3) at room temperature. 750×.

Long-time aging at 450 and 550°C had practically no effect on tensile data of specimens in the as-annealed condition. Aging of cold-worked specimens at these temperatures, however, brought about appreciable changes in tensile properties. The cold-worked structure itself is conducive to precipitation at lower temperatures, and the stored energy supplies a driving force for a change in microstructure by recovery and/or recrystallization. The variation of yield and ultimate tensile strengths with test and aging temperature in the cold-worked-and-aged specimens [Fig. 12(*a*)] is, therefore, much greater than in annealed-and-aged specimens [Fig. 7(*a*)].

Table 6. Tensile data[a] of cold-worked-and-aged[b] type 316 stainless steel at various test temperatures

Aging and test temperature (°C)	Strength (psi)		Uniform plastic strain (%)	Elongation (%)
	Yield (0.2% offset)	Ultimate tensile		
	$\times 10^3$	$\times 10^3$		
450	114.5	118.2	0.6	4.7
550	90.5	96.9	2.3	8.0
650	43.4	50.0	5.1	24.8

[a]Tested at a crosshead speed of 0.002 in./min.

[b]Swaged at room temperature (20% reduction in area) and aged 4000 hr at the test temperature.

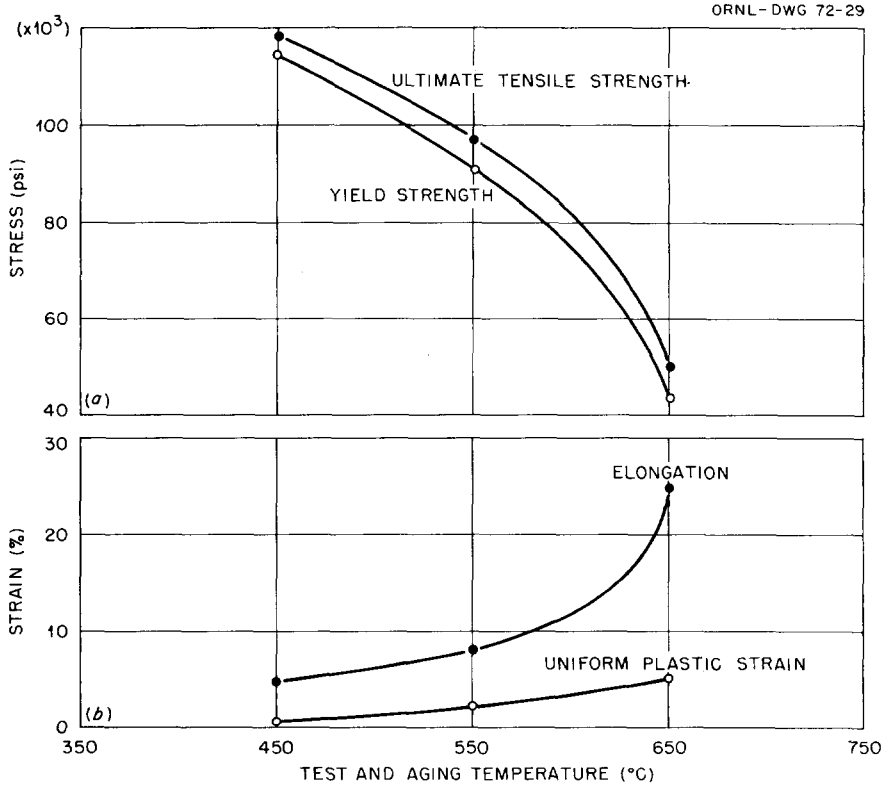

Fig. 12. Effect of test-and-aging temperature on (*a*) ultimate tensile and yield strengths, and (*b*) elongation and uniform plastic strain of type 316 stainless steel cold worked to a 20% reduction in area at room temperature, aged 4000 hr, and then tested at a crosshead speed of 0.002 in./min at the aging temperatures.

While the work-hardening rates in the cold-worked-and-aged specimens were as low as in the unaged cold-worked specimens, the strength level decreased significantly, and the rate of loss of yield and ultimate tensile strengths with increasing test-and-aging temperature was higher for the cold-worked-and-aged [Fig. 12(*a*)] than for the as-cold-worked condition [Fig. 10(*a*)]. This was due to more extensive recovery and precipitation, and, at 650°C, even partial (20%) recrystallization. Electron micrographs depicting the microstructure of the unstrained portion of cold-worked specimens aged and tested at 450, 550, and 650°C substantiate this (Fig. 13).

A comparison of the elongation values of aged and unaged cold-worked specimens shows that test temperatures up to 550°C do not affect elongation in unaged specimens [Fig. 10(*b*)], but the effect of long-time aging is revealed in the continuous increase in elongation with test-and-aging temperature [Fig. 12(*b*)].

Long-time aging of as-annealed specimens led to a decrease in ultimate tensile strength and an increase in yield strength (because of precipitates) as the test-and-aging temperature increased [Fig. 7(*a*)]. For cold-worked specimens both yield and ultimate tensile strengths, though at a higher level, decreased with increasing test-and-aging temperature [Fig. 12(*a*)]. Since the drop in strength with test-and-aging temperature was much larger for the previously cold-worked than for the annealed specimens, the ultimate tensile strengths were the same for the annealed-and-aged and the cold-worked-and-aged specimens when aged and tested at 650°C. The yield strength of the cold-worked-and-aged specimen was still higher at 650°C than that of the annealed-and-aged specimens. However, an extrapolation of the respective curves in Figs. 7(*a*) and 12(*a*) seems to indicate that an annealed specimen aged 4000 hr and tested at about 675 or 700°C would have a higher yield strength than a cold-worked specimen tested and aged at the same temperature.

A comparison of the microstructures of the unstrained portion of specimens that have been annealed and cold worked and subsequently aged for 4000 hr at 650°C (Fig. 14) makes the above prediction appear plausible. The precipitate structure of the annealed-and-aged specimen, crystallographically related to the matrix, suggests a higher yield strength than the morphologically different precipitate structure of the cold-worked-and-aged specimen (partially recrystallized), which is characterized by large σ-phase particles.

Although the annealed-and-aged specimen derives its strength from its precipitate structure, the yield strength of the cold-worked-and-aged specimen at 650°C is due to the remaining 80% of cold-worked and recovered microstructure. A small increase in test-and-aging temperature would lead to complete recrystallization in the originally cold-worked specimen and, therefore, drastically lower its yield strength, while such an increase in test-and-aging temperature would be expected to affect the precipitate structure of an annealed-and-aged specimen to a much lesser degree.

Thus, cold work seems to favor formation of σ phase and will, on aging at temperatures above 650°C, produce precipitate structures that are inferior in strength and ductility to those obtained by aging annealed specimens. The accelerating effect of cold work on the formation of σ phase is well documented,[11–14] and Weiss and Stickler's[14] time-temperature precipitation (TTP) diagram for as-annealed type 316 stainless steel indicates that an aging treatment of 4000 hr at 650°C should not lead to any substantial formation of σ phase. Cold work before aging, however, usually shifts the various precipitation reactions to shorter times and lower temperatures, so the above aging treatment (4000 hr at 650°C) would fall within the region of σ phase formation outlined by the TTP diagram. Thus, the difference in precipitate structures between

11. P. A. Benkinsop and J. Nutting, *J. Iron Steel Inst.* **205**, 953–58 (1967).
12. P. Duhay, J. Ivan, and E. Makovický, *J. Iron Steel Inst.* **206**, 1245–51 (1968).
13. P. K. Koh, *J. Metals* **5**, 339–43 (1953).
14. B. Weiss and R. Stickler, *Met. Trans.* **3**, 851–66 (1972).

annealed-and-aged and cold-worked-and-aged specimens, as shown in Fig. 14, could have been predicted on the basis of Weiss and Stickler's TTP diagram.

Short-time aging. Room-temperature tensile data of specimens reduced 20% in area by swaging at room temperature and aged for 10 hr at 450, 550, 650, and 750°C are listed in Table 7.

Although aging for 4000 hr at 450 and 550°C affected the tensile properties of cold-worked specimens, an aging time of only 10 hr does not result in any significant tensile property changes. Figure 15(*a*) shows that both yield and ultimate tensile strengths change markedly only at aging temperatures above 550°C.

Fig. 13. Electron micrographs showing the microstructure of type 316 stainless steel cold worked to a 20% reduction in area at room temperature and aged 4000 hr at (*a*) 450, (*b*) 550, and (*c*) 650°C.

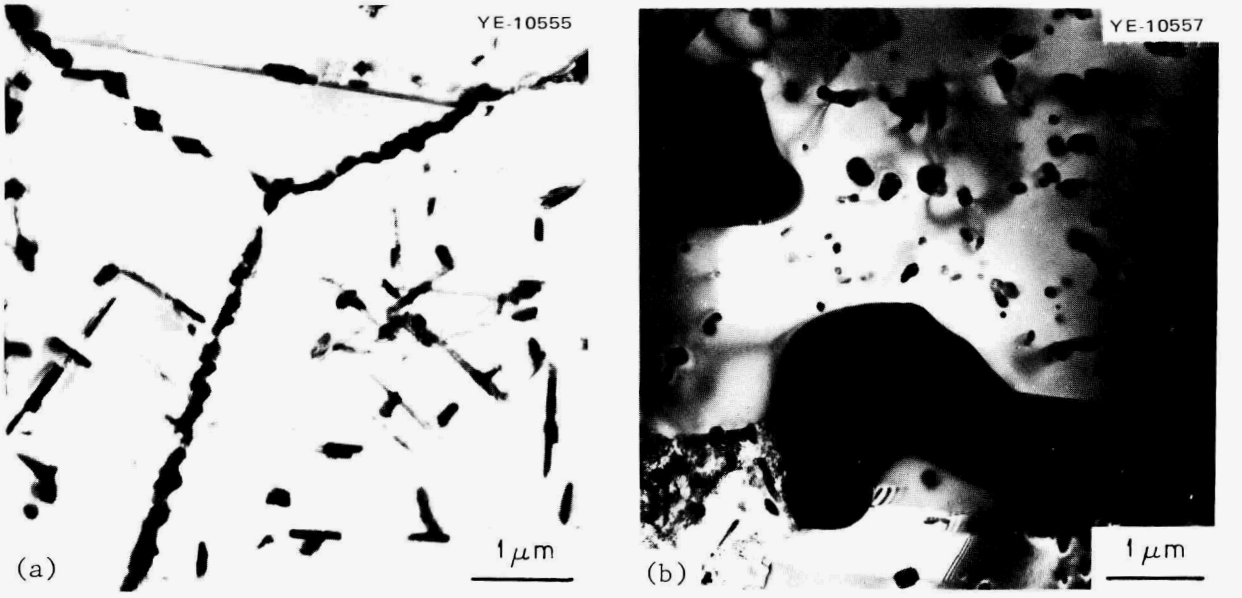

Fig. 14. Electron micrographs showing the microstructure of type 316 stainless steel aged 4000 hr at 650°C after being (*a*) annealed 1 hr at 1050°C and (*b*) cold worked to a 20% reduction in area at room temperature.

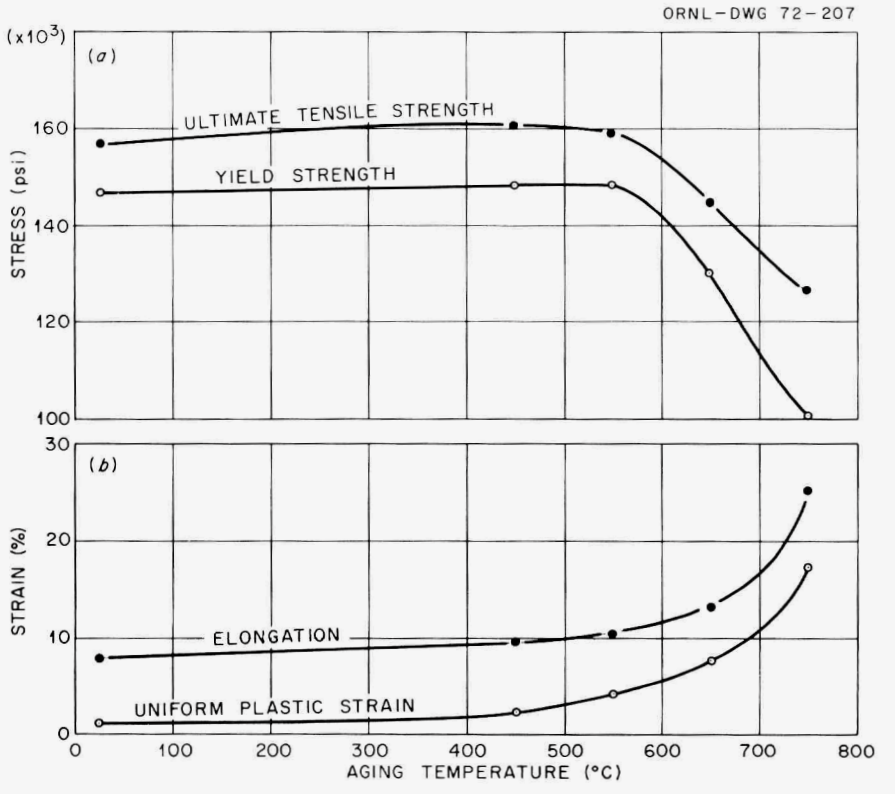

Fig. 15. Effect of aging temperature on (*a*) ultimate tensile and yield strengths, and (*b*) elongation and uniform plastic strain of type 316 stainless steel cold worked to a 20% reduction in area at room temperature, aged for 10 hr and tested at room temperature at a crosshead speed of 0.002 in./min.

Recovery during aging for 10 hr at 650°C clearly affected the microstructure [Fig. 16(*c*)] and the mechanical properties (Fig. 15), and an aging temperature of 750°C led to a completely recrystallized specimen [Fig. 16(*d*)]. Figure 15(*b*) shows that both elongation and uniform plastic strain increased by about the same amount as the aging temperature was increased. Microstructures resulting from the various aging treatments, from the as-cold-worked up to the fully recrystallized condition, are shown in Fig. 16.

Effect of Different Amounts of Tensile Prestrain on Post-Aging Tensile Data

Tensile data of specimens prestrained in tension and subsequently aged for 4000 hr at 650°C are listed in Table 8. Small increases in tensile prestrain at room temperature before aging 4000 hr at 650°C led to small increases in yield and ultimate tensile strengths [Fig. 17(*a*)] and decreases in uniform plastic strain [Fig. 17(*b*)] at 650°C.

A comparison of tensile data between a specimen prestrained 20% in tension and another one reduced 20% in area by swaging shows that not only the yield and ultimate tensile strengths but also uniform plastic strain and elongation are lower for the swaged specimen than for the specimen prestrained in tension (Fig. 17). This is most likely due to the different kinds of deformation resulting in different amounts of cold

Table 7. Room-temperature tensile data[a] of cold-worked-and-aged[b] type 316 stainless steel

Pretest aging treatment	Strength (psi)		Uniform plastic strain (%)	Elongation (%)
	Yield (0.2% offset)	Ultimate tensile		
	$\times 10^3$	$\times 10^3$		
None	146.9	156.8	1.1	8.1
10 hr at 450°C	148.7	161.0	2.3	9.6
10 hr at 550°C	148.6	159.2	4.1	10.3
10 hr at 650°C	130.2	144.8	7.6	13.2
10 hr at 750°C	100.7	126.7	17.1	24.9

[a]Tested at a crosshead speed of 0.002 in./min.
[b]Swaged at room temperature (20% reduction in area).

Table 8. Tensile data[a] of prestrained-and-aged[b] type 316 stainless steel

Tensile prestrain (%)	Strength (psi)		Uniform plastic strain (%)	Elongation (%)
	Yield (0.2% offset)	Ultimate tensile		
	$\times 10^3$	$\times 10^3$		
0	26.9	48.1	11.7	36.8
5	35.7	54.4	10.3	40.6
10	38.9	54.6	8.8	33.1
20	46.6	57.8	6.6	33.7

[a]Tested at 650°C and a crosshead speed of 0.002 in./min.
[b]Prestrained at room temperature and aged for 4000 hr at 650°C.

work and, possibly, different grain orientation. Since partial (~20%) recrystallization took place during aging of the specimen reduced 20% in area by swaging, the difference in yield and ultimate tensile strengths may well be due to different degrees of pretest recrystallization, expected to be less for the specimen prestrained 20% in tension. At lower prestrains, recrystallization may not take place at all.

The lower elongation and uniform plastic strain values for the specimen reduced 20% in area by swaging, as compared with the specimen 20% prestrained in tension, may well be explained by the difference in directionality of the deformation process. Grains and hence grain boundary precipitates are likely to be oriented differently with respect to the direction of the tensile stress.

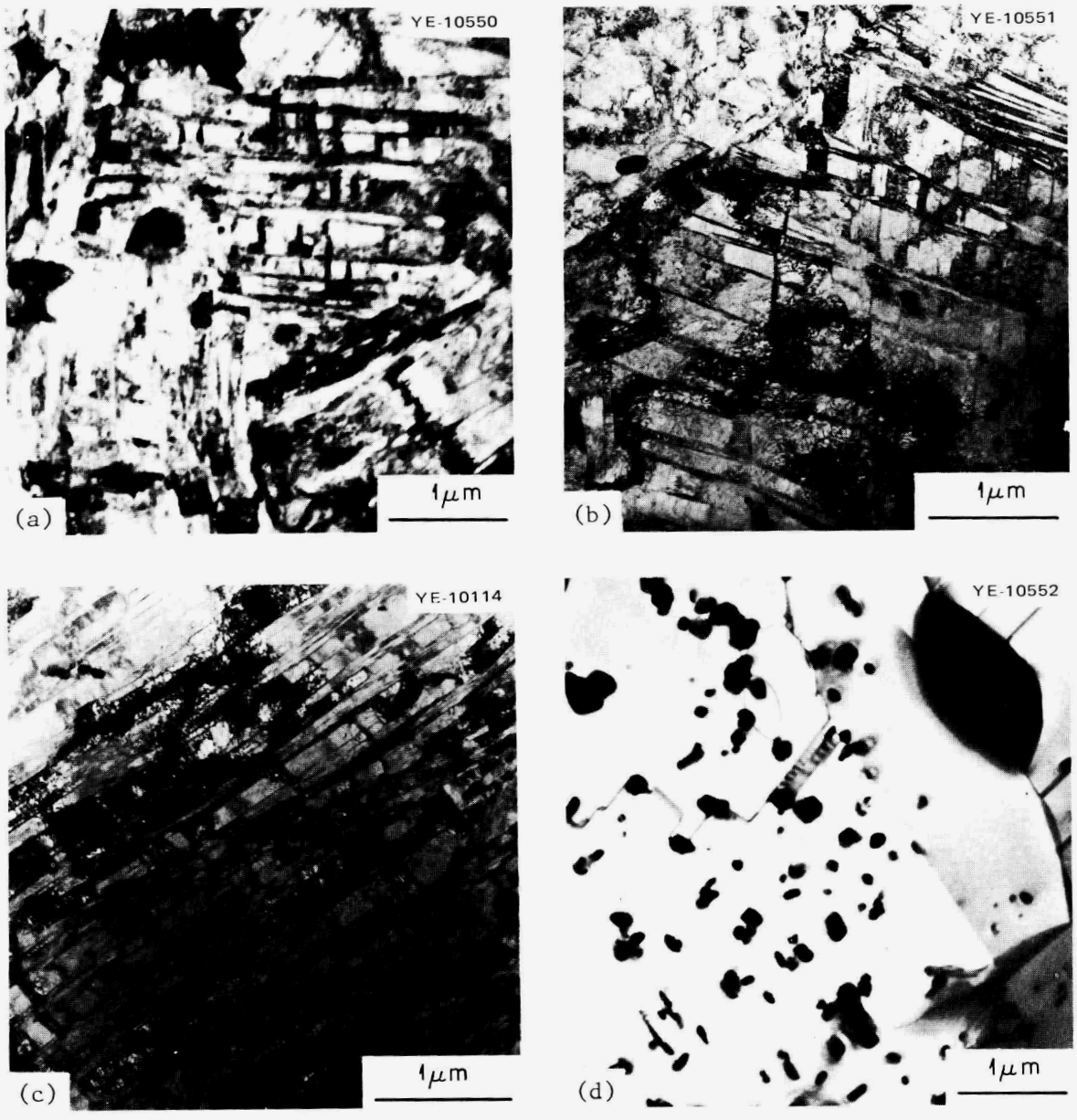

Fig. 16. Electron micrographs showing the microstructure of type 316 stainless steel reduced 20% in area by swaging at room temperature in (*a*) the as-cold-worked condition, and cold-worked-and-aged conditions: aged 10 hr at (*b*) 550, (*c*) 650, and (*d*) 750°C.

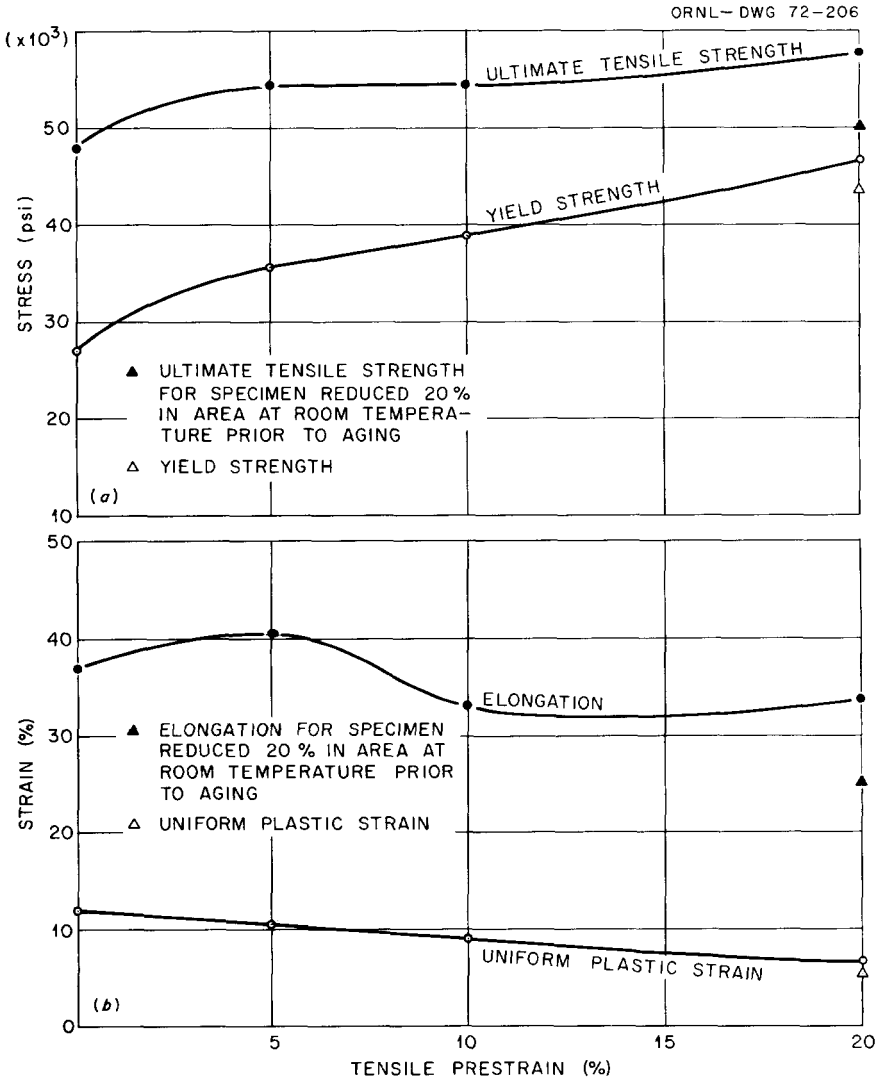

Fig. 17. Effect of tensile prestrain on (*a*) ultimate tensile and yield strengths, and (*b*) elongation and uniform plastic strain of type 316 stainless steel prestrained at room temperature, aged 4000 hr at 650°C, and tested at a crosshead speed of 0.002 in./min at 650°C.

No serrations were observed in the stress-strain curves of the above specimen, in agreement with other findings and with the low work-hardening rate.

SUMMARY

A detailed qualitative analysis of the stress-strain behavior of type 316 stainless steel has been made on the basis of stress-strain curves, their shapes, and serrations occurring in them. The serrations observed could be classified into three types (A, B, and C) occurring at different temperatures, strains, and strain rates. For a given strain and crosshead speed, type A occurs at a lower temperature than types B and C, and type B at a lower temperature than type C. The serrations are due to interactions between solute atoms (carbon and nitrogen) and mobile dislocations. These interactions strongly affect the work-hardening rate and thus the ultimate tensile strength and the uniform plastic strain values.

Variations in crosshead speed, which had little or no effect on the yield strength, resulted, however, in changes in ultimate tensile strength and uniform plastic strain during tests at 650°C because of the diffusion-dependent, and thus time-dependent, characteristics of the above interactions. Changes in test temperature between 450 and 650°C affected tensile properties in a manner similar to variations in crosshead speed within that temperature range. As-annealed, annealed-and-aged, cold-worked (20%), and cold-worked-and-aged specimens were studied. Specimens aged for 4000 hr were tested at their respective aging temperatures. Between 450 and 550°C, long-time aging had practically no effect on the properties of annealed specimens, while cold-worked specimens showed a significant response to aging at these temperatures. No precipitation occurred during aging at 450°C in the annealed specimens, while aging at 550°C resulted in grain boundary precipitates. At 650°C, precipitates were found within the grains and at their boundaries. The precipitate structure of the annealed specimens aged at 650°C was significantly different from that observed in the recrystallized portion (~20%) of cold-worked specimens aged at the same temperature. The yield strength of the annealed specimens increased with increasing test-and-aging temperature because of the above precipitate structure, while recovery and recrystallization led to a decrease in yield strength of cold-worked specimens as the test-and-aging temperature increased. Cold work facilitated precipitation and the formation of large σ-phase particles during subsequent aging. No such σ-phase particles were observed in annealed specimens after an aging treatment of 4000 hr at 650°C.

For aging times of only 10 hr, significant changes in room-temperature tensile data of cold-worked specimens were observed only after aging above 550°C. Aging for 10 hr at 750°C led to a completely recrystallized microstructure.

Specimens cold worked by prestraining in tension at room temperature yielded results different from those of specimens reduced by swaging at room temperature after long-time aging at 650°C when tested at that temperature. Thus 20% elongation cannot be equated to 20% reduction in area in terms of the resulting dislocation density, and the difference in the deformation direction leads to different textures.

ACKNOWLEDGMENTS

The author would like to acknowledge the assistance of F. L. Beeler and L. G. Rardon in performing the mechanical property tests, and thank R. W. Carpenter and J. E. Spruiell for their valuable suggestions made on reviewing the manuscript.

INTERNAL DISTRIBUTION
(77 copies)

(3) Central Research Library
ORNL – Y-12 Technical Library,
Document Reference Section
(10) Laboratory Records Department
Laboratory Records, ORNL R.C.
ORNL Patent Office
G. M. Adamson, Jr.
E. E. Bloom
R. W. Carpenter
J. E. Cunningham
(5) D. Fahr
M. H. Fontana
R. J. Gray
B. L. Greenstreet
W. O. Harms
(3) M. R. Hill
F. J. Homan
P. R. Kasten
J. M. Leitnaker
E. L. Long, Jr.
(5) W. R. Martin
H. E. McCoy, Jr.
H. C. McCurdy
C. J. McHargue
R. B. Parker
P. Patriarca
C. E. Pugh
P. L. Rittenhouse
G. M. Slaughter
J. O. Stiegler
R. W. Swindeman
D. B. Trauger
W. E. Unger
T. N. Washburn
J. R. Weir, Jr.
G. D. Whitman

Subcontractors and Consultants

Atomics International, P.O. Box 309, Canoga Park, CA 91304
R. I. Jetter

Babcock & Wilcox Company, P.O. Box 835, Alliance, OH 44601
W. E. Leyda
C. C. Schultz
D. B. Van Fossen

Battelle Memorial Institute, 505 King Avenue, Columbus, OH 43201
C. E. Jaske
E. C. Rodabaugh
G. H. Workman

Brown University, Providence, RI 02912
W. N. Findley

The Catholic University of America, Washington, DC 20017
A. J. Durelli

Cornell University, Department of Materials Science and Engineering, Ithaca, NY 14850
G. V. Smith

E. P. Esztergar, 7993 Prospect Place, La Jolla, CA 92037

Franklin Institute Research Laboratories, The Benjamin Franklin Parkway, Philadelphia, PA 19103
Zenons Zudans

General Electric Company, 175 Curtner Ave., San Jose, CA 95125
Y. R. Rashid

Pennsylvania State University, University Park, PA 16802
S. Y. Zamrick

Teledyne Materials Research Company, 303 Bear Hill Road, Waltham, MA 02154
T. Branca
W. E. Cooper
J. L. McLean

University of California, Lawrence Radiation Laboratory, Inorganic Materials Research Division, Berkeley, CA 94720
Leo Brewer

University of California, Revelle College, Department of Physics, P.O. Box 109, La Jolla, CA 92037
Walter Kohn

University of Illinois, Department of Physics, Urbana, IL 61801
W. S. Williams

University of Tennessee, Department of Chemical and Metallurgical Engineering, Knoxville, TN 37916
J. E. Spruiell

EXTERNAL DISTRIBUTION
(306 copies)

USAEC DIVISION OF REACTOR RESEARCH AND DEVELOPMENT, Washington, D.C. 20545
(2) Director

USAEC-RRD SENIOR SITE REPRESENTATIVE, Oak Ridge National Laboratory, Oak Ridge, TN 37830

USAEC OAK RIDGE OPERATIONS OFFICE, P.O. Box E, Oak Ridge, TN 37830
Research and Technical Support Division

USAEC TECHNICAL INFORMATION CENTER, Office of Information Services, P.O. Box 62, Oak Ridge, TN 37830

(302) For distribution as shown in TID-4500 Distribution Category UC-79b (Fuels and Materials Engineering Development); UC-79h (Structural Materials and Design Engineering); UC-79k (Components)

☆U.S. GOVERNMENT PRINTING OFFICE: 1973-747-302/67